

Third harmonic generation in gapped bilayer graphene

A.K. Avetissian, A.G. Ghazaryan, and Kh. V. Sedrakian

Centre of Strong Fields, Yerevan State University, 1 A. Manukian, Yerevan 0025, Armenia

(Dated: May 21, 2019)

With the help of numerical simulations in microscopic nonlinear quantum theory of coherent electromagnetic radiation interaction with a gapped bilayer graphene, we find out the optimal values of pump wave intensity, graphene temperature, and energy gap induced by a constant electric field for practically significant third order harmonic coherent emission. The Liouville-von Neumann equation is treated numerically for the third harmonic generation in multiphoton excitation regime near the Dirac points of the Brillouin zone. We examine the rates of the third harmonic at the particle-hole annihilation in the field of a strong pump wave of linear polarization for practically real/optimal parameters of a considering system. The obtained results show that by choosing the optimal values of the main characteristic parameters, a gapped bilayer graphene can serve as an effective medium for generation of the third harmonic at room temperatures in the terahertz and far infrared domains.

PACS numbers: 78.67.Wj, 42.50.Hz, 78.47.jh, 03.65.Pm

I. INTRODUCTION

Recently the interest has grown to harmonics generation and related multiphoton processes in graphene and other 2D nanostructures with the similar properties [1–21] due to the achievements of production of new nanomaterials. Many experiments already exist where the theoretical predictions have been justified, in particular, the experiment [17] with generation of 9th harmonic in graphene in infrared regime, and generation of harmonics extending to the 13th order in 2D semiconductor [22] and in solids [23]. In these nanostructures at very high carrier mobility, with increasing pump wave intensity one can achieve an ultrafast excitation regime and it is important that threshold values of intensities of electromagnetic (EM) radiation for observation of nonlinear phenomena compared with free electrons and atoms are essentially reduced. In particular, for the infrared photons one can obtain nonlinear effects at the 10^9 times smaller intensities of an external EM field [24].

Bilayer graphene (*AB* stacked) [2, 9, 25, 26] (as the other multilayer 2D nanostructures [1–5]) is of great interest since its electronic states are considerably richer than those of a monolayer graphene [27–30]. But both single- and multilayer graphene in their unperturbed state lack the band gap [31, 32]. However, multilayer graphene materials under the application of a perpendicular electric field may exhibit the ability to produce an electrically tunable band gap. These outcomes disclose new possibilities of a much wider range of applications for graphene materials in electronics and photonics [27, 33–36]. Moreover, in the case of *AB* stacked bilayer graphene the trigonal warping effect for the energy spectrum deforms the low-energy excitation with $\mathcal{E} \lesssim 10$ meV, which significantly enhances the rates of the harmonics [9] in the terahertz region compared to a monolayer graphene. It takes place the modification of quasi-energy spectrum, in particular, the induction of valley polarized currents [37, 38], as well as second- and third-order nonlinear-optical effects [39–43] in *AB* stacked bilayer graphene under the applied intense EM field. So, bilayer graphene (*AB* stacked) has some advantage as compared to a single layer graphene for the photonic applications because of its anisotropic zone structure and the extensive tunable band gap [25, 26, 44–50]. The large tunable band gaps with maximal energy $U \simeq 280$ meV [35] can make possible to control nonlinear EM response in bilayer graphene at room temperatures, which is impossible in intrinsic graphene [9].

The aim of the current paper is to find out optimal parameters of light-gapped bilayer graphene interaction for third order harmonic radiation. We investigate third order harmonic radiation efficiency depending on the value of energy gap, temperature, pump wave frequency, and intensity. The consideration is based on the solution of the Liouville-von Neumann equation for density matrix in multiphoton excitation regime near the Dirac points of the Brillouin zone. We show that there is an extensive emission (coherent) of the third harmonic at the wave-induced particle or hole acceleration and annihilation. We have revealed the optimal conditions for third harmonic generation.

The paper organization is the following. In Sec. II the equations for a single-particle density matrix is numerically solved in the multiphoton interaction regime. In Sec. III, the problem of third order harmonic generation at the multiphoton excitation of gapped bilayer graphene is considered. The conclusions are given in Sec. IV.

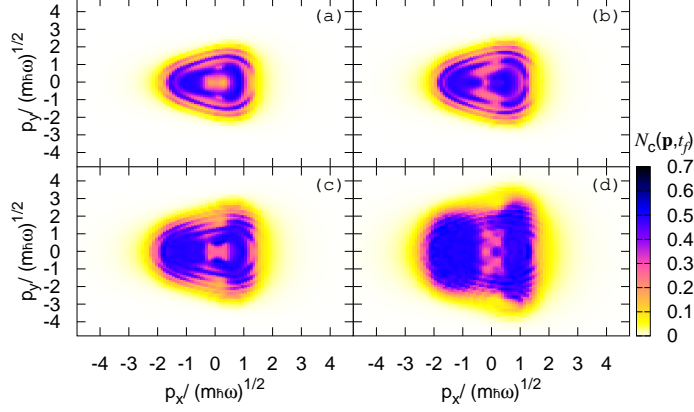


FIG. 1: (Color online) Creation of a particle-hole pair in bilayer graphene at multiphoton resonant excitation with the trigonal warping effect for middle gap energy $U = 0.1$ eV. Particle distribution function $N_c(\mathbf{p}, t_f)$ (in arbitrary units) after the interaction is displayed at various wave frequencies: (a) $\omega = 0.06$ eV/ \hbar , (b) $\omega = 0.05$ eV/ \hbar , (c) $\omega = 0.04$ eV/ \hbar , and (d) $\omega = 0.03$ eV/ \hbar . The temperature is taken to be $T = 0.025$ eV, the wave intensity is $I_\chi = 7.5 \times 10^6$ Wcm $^{-2}$. The results are for the valley $\zeta = 1$.

II. BASIC MODEL AND THEORY

Back to the issue of the third harmonic radiation let us choose initially the interaction parameters as follow. At an intraband transitions the interaction of a particle with the wave at the photon energies $\hbar\omega > \mathcal{E}_L$ [9] characterizes by the known dimensionless parameter χ :

$$\chi = eE_0/(\omega\sqrt{m\hbar\omega}), \quad (1)$$

where E_0 is a wavestrength, ω is a wavefrequency, e is an electron charge and m is an effective mass. Moreover, due to the gap the interband transitions are characterized by so-called Keldysh [51] parameter

$$\gamma = \omega\sqrt{mU}/(eE_0) = \chi^{-1}\sqrt{U/(\hbar\omega)}. \quad (2)$$

Here U is a band gap energy, \mathcal{E}_L is the Lifshitz energy, \hbar is the Planck constant. The last defines the tunneling ($\gamma \ll 1$) or multiphoton ($\gamma \gg 1$) character of the ionization process in the strong laser field. For the considered case, the ionization process reduces to the transfer of the electron from the valence band into the conduction band that is the creation of an electron-hole pair. Since the interband transitions can be neglected when $\gamma \gg 1$, then the wave field cannot provide enough energy for the creation of an electron-hole pair, and the generation of harmonics is suppressed. If $\gamma \sim 1$ or $\gamma \ll 1$, interband transitions take place. In the current paper, we will consider the nonadiabatic regime for the generation of third harmonic at $\chi \sim 1$ and $\gamma \sim 1$.

Let us investigate the multiphoton excitations of Fermi-Dirac sea in the gapped bilayer graphene in nonadiabatic regime. In accordance with the microscopic nonlinear quantum theory of AB stacked gapped bilayer graphene, the low-energy excitations $|\mathcal{E}_\sigma| < \gamma_1 \simeq 0.39$ eV in the immediate vicinity of the Dirac points K_ζ (valley quantum number $\zeta = \pm 1$) one can describe by the effective single particle Hamiltonian [27–29]:

$$\hat{H}_\zeta = \begin{pmatrix} \frac{U}{2} & h_\zeta^*(\mathbf{p}) \\ h_\zeta(\mathbf{p}) & -\frac{U}{2} \end{pmatrix}. \quad (3)$$

Here $\hat{\mathbf{p}} = \{\hat{p}_x, \hat{p}_y\}$ is the electron momentum operator, $m = \gamma_1/(2v_F^2)$ is the effective mass (v_F is the Fermi velocity in a monolayer graphene); $v_3 = \sqrt{3}b\gamma_3/(2\hbar)$ is the effective velocity related to oblique interlayer hopping $\gamma_3 = 0.32$ eV ($b \approx 0.246$ nm is the distance between the nearest A sites); and

$$h_\zeta(\mathbf{p}) = -\frac{1}{2m}(\zeta\hat{p}_x + i\hat{p}_y)^2 + v_3(\zeta\hat{p}_x - i\hat{p}_y). \quad (4)$$

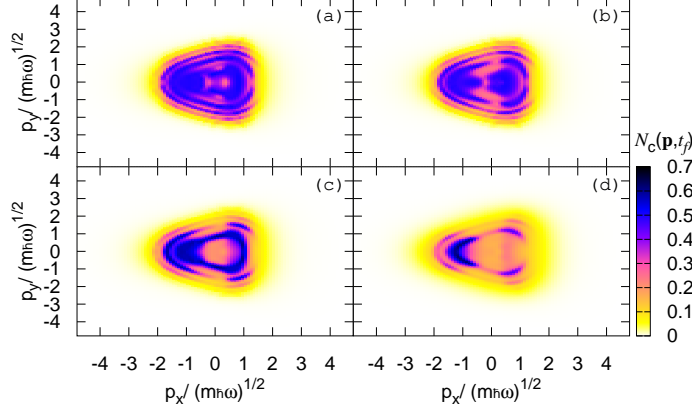


FIG. 2: (Color online) The same as Fig. 1 but for fixed dimensionless intensity parameter $\chi = 1$. The results are for the valley $\zeta = 1$: (a)–(d) correspond to the photon energy $\hbar\omega/eV = 0.06, 0.05, 0.04$ and 0.03 , respectively.

The diagonal elements in Eq. (3) correspond to induced by perpendicular to graphene plane electric field gap U . The first term in Eq. (4) gives a pair of parabolic bands $E = \pm p^2/(2m)$, and the second term connects with γ_3 causes trigonal warping in the band dispersion. The Lifshitz transition (separation of the Fermi surface) in the low-energy region occurs at an energy $\mathcal{E}_L = mv_3^2/2 \simeq 1$ meV, and the two touching parabolas are transformed into the four separate “pockets” [9]. The spin and the valley quantum numbers are conserved. There is no degeneracy upon the valley quantum number ζ . Since there are no intervalley transitions, the valley index ζ one has considered as a parameter.

The eigenstate functions of the effective Hamiltonian (3) are the spinor ones,

$$\Psi_\sigma(\mathbf{r}) = \frac{1}{\sqrt{S}}|\sigma, \mathbf{p}\rangle e^{i\mathbf{p}\cdot\mathbf{r}} \quad (5)$$

with

$$|\sigma, \mathbf{p}\rangle = \frac{1}{\sqrt{S}}\sqrt{\frac{\mathcal{E}_\sigma + \frac{U}{2}}{2\mathcal{E}_\sigma}} \begin{pmatrix} 1 \\ \frac{1}{\varepsilon_\sigma + \frac{U}{2}}\Gamma(\mathbf{p}) \end{pmatrix}. \quad (6)$$

Here

$$\mathcal{E}_\sigma(\mathbf{p}) = \sigma\sqrt{\frac{U^2}{4} + (v_3p)^2 - \zeta\frac{v_3p^3}{m}\cos 3\vartheta + \left(\frac{p^2}{2m}\right)^2}; \quad (7)$$

are the corresponding eigenenergies, and

$$\Gamma(\mathbf{p}) = -\frac{p^2}{2m}e^{i2\zeta\vartheta} + \zeta v_3 p e^{-i\zeta\vartheta}, \quad (8)$$

$\vartheta = \arctan(p_y/p_x)$, S is the quantization area, and σ is the band index: $\sigma = 1$ and $\sigma = -1$ for conduction and valence bands.

To exclude the effect of the magnetic field, the EM wave propagates in the perpendicular direction to the gapped bilayer graphene sheets (XY). A plane quasimonochromatic EM wave is taken to be linearly polarized along the Y axis:

$$\mathbf{E}(t) = f(t) E_0 \hat{\mathbf{y}} \sin \omega t. \quad (9)$$

The wave slowly varying envelope $f(t)$ is defined by the function:

$$f(t) = \begin{cases} \sin^2(\pi t/\mathcal{T}_p), & 0 \leq t \leq \mathcal{T}_p, \\ 0, & t < 0, t > \mathcal{T}_p, \end{cases}, \quad (10)$$

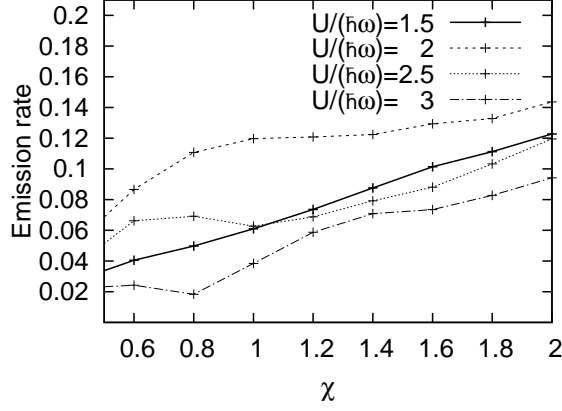


FIG. 3: Third harmonic emission rate J_3 (in arbitrary units) for gapped bilayer graphene versus χ for various band gaps. The temperature is taken to be $T = 0.025$ eV, wave frequency is $\omega = 0.05$ eV/ \hbar .

where $\mathcal{T}_p = 20\mathcal{T}$ is the pulse duration, and $\mathcal{T} = 2\pi/\omega$.

By the second quantization formalism, the fermionic field operator, expanding on the basis of free states (5), can be written in the form:

$$\widehat{\Psi}(\mathbf{r}, t) = \sum_{\mathbf{p}, \sigma} \widehat{a}_{\mathbf{p}, \sigma}(t) \Psi_{\sigma}(\mathbf{r}). \quad (11)$$

Here $\widehat{a}_{\mathbf{p}, \sigma}(t)$ and $\widehat{a}_{\mathbf{p}, \sigma}^+(t)$ are the annihilation and creation operators for an electron with the momentum \mathbf{p} , which satisfy the fermionic anticommutation rules at equal times. The single-particle Hamiltonian in the presence of a uniform time-dependent electric field $E(t)$ in a length gauge can be expressed in the form:

$$\widehat{H}_s = \widehat{H}_{\zeta} + \begin{pmatrix} e\mathbf{r}\mathbf{E}(t) & 0 \\ 0 & e\mathbf{r}\mathbf{E}(t) \end{pmatrix}. \quad (12)$$

Using the expansion (11), the second quantized total Hamiltonian can be presented in the form:

$$\widehat{H} = \sum_{\sigma, \mathbf{p}} \mathcal{E}_{\sigma}(\mathbf{p}) \widehat{a}_{\sigma\mathbf{p}}^+ \widehat{a}_{\sigma\mathbf{p}} + \widehat{H}_{\text{int}}, \quad (13)$$

where the part of interaction with the EM field is given by the relation:

$$\begin{aligned} \widehat{H}_{\text{int}} = & ie \sum_{\mathbf{p}, \mathbf{p}', \sigma} \delta_{\mathbf{p}'\mathbf{p}} \partial_{\mathbf{p}'} \mathbf{E}(t) \widehat{a}_{\mathbf{p}, \sigma}^{\dagger} \widehat{a}_{\mathbf{p}', \sigma'} \\ & + \sum_{\mathbf{p}, \sigma} \mathbf{E}(t) (\mathbf{D}_t(\sigma, \mathbf{p}) \widehat{a}_{\mathbf{p}, \sigma}^+ \widehat{a}_{\mathbf{p}, -\sigma} + \mathbf{D}_m(\sigma, \mathbf{p}) \widehat{a}_{\mathbf{p}, \sigma}^+ \widehat{a}_{\mathbf{p}, \sigma}), \end{aligned} \quad (14)$$

with the transition dipole moment

$$\mathbf{D}_t(\sigma, \mathbf{p}) = \hbar e \langle \sigma, \mathbf{p} | i\partial_{\mathbf{p}} | -\sigma, \mathbf{p} \rangle \quad (15)$$

and the mean dipole moment or Berry connection:

$$\mathbf{D}_m(\sigma, \mathbf{p}) = \hbar e \langle \sigma, \mathbf{p} | i\partial_{\mathbf{p}} | \sigma, \mathbf{p} \rangle. \quad (16)$$

The ultimate expressions of the dipole moment components are given in the Appendices by Eqs. (32)–(35).

For description of multiphoton interaction in a gapped bilayer graphene the Liouville–von Neumann equation with a single-particle density matrix

$$\rho_{\alpha, \beta}(\mathbf{p}, t) = \langle \widehat{a}_{\mathbf{p}, \beta}^+(t) \widehat{a}_{\mathbf{p}, \alpha}(t) \rangle \quad (17)$$

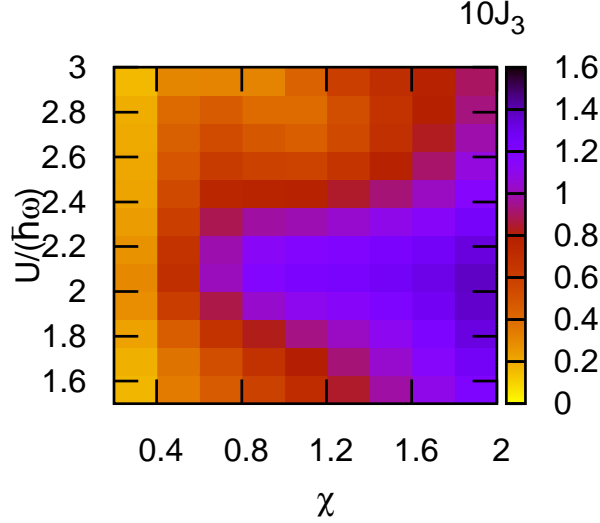


FIG. 4: 3rd harmonic emission rate in bilayer graphene at multiphoton excitation J_3 (in arbitrary units) versus the parameter χ and the gap energy $U/(\hbar\omega)$ at the same other parameters as in Fig. 3.

has the form:

$$i\hbar \frac{\partial \hat{a}_{\mathbf{p},\alpha}(t)}{\partial t} = [\hat{a}_{\mathbf{p},\alpha}(t), \hat{H}], \quad (18)$$

where $\hat{a}_{\mathbf{p},\alpha}(t)$ obeys the Heisenberg equation.

We use only the \mathbf{p} -diagonal elements of the density matrix due to the homogeneity of the problem. Since homogeneous relaxation processes are slow compared with inhomogeneous ones, the relaxation processes can be taken into Liouville–von Neumann equation including the inhomogeneous phenomenological damping term. Hence, using the Eqs. (13)–(18), we have to solve the differential equations

$$\begin{aligned} i\hbar \frac{\partial \rho_{\alpha,\beta}(\mathbf{p}, t)}{\partial t} - i\hbar e\mathbf{E}(t) \frac{\partial \rho_{\alpha,\beta}(\mathbf{p}, t)}{\partial \mathbf{p}} = \\ (\mathcal{E}_\alpha(\mathbf{p}) - \mathcal{E}_\beta(\mathbf{p}) - i\hbar\Gamma(1 - \delta_{\alpha\beta})) \rho_{\alpha,\beta}(\mathbf{p}, t) \\ + \mathbf{E}(t) (\mathbf{D}_m(\alpha, \mathbf{p}) - \mathbf{D}_m(\beta, \mathbf{p})) \rho_{\alpha,\beta}(\mathbf{p}, t) \\ + \mathbf{E}(t) [\mathbf{D}_t(\alpha, \mathbf{p}) \rho_{-\alpha,\beta}(\mathbf{p}, t) - \mathbf{D}_t(-\beta, \mathbf{p}) \rho_{\alpha,-\beta}(\mathbf{p}, t)], \end{aligned} \quad (19)$$

where Γ is the damping rate. The particle distribution functions for the conduction $N_c(\mathbf{p}, t) = \rho_{1,1}(\mathbf{p}, t)$ and valence $N_v(\mathbf{p}, t) = \rho_{-1,-1}(\mathbf{p}, t)$ bands correspond to diagonal elements. The nondiagonal elements are interband polarization $\rho_{1,-1}(\mathbf{p}, t) = P(\mathbf{p}, t)$ and its complex conjugate $\rho_{-1,1}(\mathbf{p}, t) = P^*(\mathbf{p}, t)$.

As an initial state, we present an ideal Fermi gas in equilibrium state with the chemical potential to be zero. We need to solve the set of Eqs. (19), and followed from the last closed set of differential equations (29)–(31) given in the Appendices for the quantities $N_v(\mathbf{p}, t)$, $N_c(\mathbf{p}, t)$, $P(\mathbf{p}, t)$, taking into account the initial conditions:

$$P(\mathbf{p}, 0) = 0; N_c(\mathbf{p}, 0) = \frac{1}{1 + e^{\varepsilon_1(\mathbf{p})/T}}, \quad (20)$$

$$N_v(\mathbf{p}, 0) = 1 - N_c(\mathbf{p}, 0), \quad (21)$$

where T is the temperature in energy units.

For the numerical solution of the set of equations (29)–(31) we transformed to the equations with partial derivatives into the ordinary ones. We changed the variables by new ones t and $\tilde{\mathbf{p}} = \mathbf{p} - \mathbf{p}_E(t)$, where $\mathbf{p}_E(t) = -e \int_0^t \mathbf{E}(t') dt$.

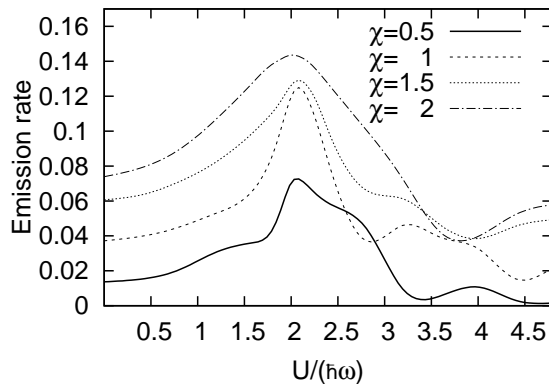


FIG. 5: 3rd harmonic emission rate in bilayer graphene J_3 (in arbitrary units), as a function of the gap energy scaled to photon energy for various wave intensities. The temperature is taken to be $T = 0.025$ eV. The wave frequency is $\omega = 0.05$ eV/ \hbar .

The last is the classical momentum given by the wave field, which with the Keldish parameter (2) and wave intensity characterize the intraband transitions. The integration of equations (29)–(31) is performed on a homogeneous grid of 10^4 $(\tilde{p}_x, \tilde{p}_y)$ -points. For the maximal momentum we take $\tilde{p}_{\max}/\sqrt{m\hbar\omega} = 5$. The time integration is performed by the fourth-order adaptive Runge-Kutta method. The relaxation rate is given $\Gamma = 0.5\mathcal{T}^{-1}$.

For all calculations an EM wave is taken to be linearly polarized along the Y axis with frequencies in terahertz domain (1.24 – 124 meV). Similar calculations for a wave linearly polarized along the X axis show qualitatively the same picture. Note that the intensity of the wave can be estimated as

$$I_\chi = \chi^2 \times 6 \times 10^{10} \text{Wcm}^{-2} (\hbar\omega/\text{eV})^3, \quad (22)$$

so the the multiphoton effects at $\chi \simeq 1$ for terahertz frequencies become essential at $I_\chi = 10^2 - 10^8 \text{Wcm}^{-2}$. If in case of $\gamma \ll 1$ the process of tunneling transitions is independent on the wave frequency, in considered cases the value I_χ required for the nonlinear regime strongly depends on the photon energy. The case of multiphoton transitions, depending on the wave frequency is considered separately.

In Figs. 1, 2, the photoexcitations of the Fermi-Dirac sea are presented at room temperatures. In Fig. 1, the density plot of the particle distribution function $N_c(\mathbf{p}, t_f)$ is shown as a function of the scaled dimensionless momentum components after the interaction at the same wave intensity I_χ for various frequencies. The pulse duration is $\mathcal{T}_p = 20\mathcal{T} \approx 1.6$ ps, and the intensity is taken to be same: $I_\chi \simeq 10^7 \text{Wcm}^{-2}$. We have taken the middle band gap $U \simeq 0.1$ eV, because as seen from similar calculations for a large band gap, with the increase of U we approach to perturbation regime at $\gamma > 1$, and only a weak excitation of Fermi-Dirac sea is appeared. In Fig. 2, for the various pump wave frequencies the photoexcitation dependence on the pump wave intensity is presented at the same dimensionless intensity parameter $\chi = 1$, for the same other parameters (U, T) as in Fig. 1. In viewed figures with the legible trigonal warping effect, describing the deviation of the excited iso-energy contours from circles, at the values of $\chi \gtrsim 1$ when $\gamma \simeq 1$ the multiphoton excitations have clearly seen. As is known, the multiphoton excitation of the Fermi-Dirac sea takes place along the trigonally warped isolines of the quasienergy $\mathcal{E}_1(\tilde{\mathbf{p}} + \mathbf{p}_E(t), t)$ spectrum modified by the wave field. Thus, the multiphoton probabilities of particle-hole pair production will have maximal values for the iso-energy contours defined by the resonant conditions: $\mathcal{T}^{-1} \int_0^{\mathcal{T}} 2\mathcal{E}_1(\tilde{\mathbf{p}} + \mathbf{p}_E(t), t) dt = n\hbar\omega$ (n is a natural number). Further,

Figs. 1, 2 demonstrate the Fermi-Dirac sea photoexcitations strong dependence on the pump wave frequency. As is seen from the last considerations, in Fig. 1 with a fixed pump wave intensity (22) the states with absorption of more photons are appearing in the Fermi-Dirac sea with decreasing of the wave frequency. The last takes place with increasing of the wave frequency in Fig. 2 when the dimensionless intensity parameter is fixed.

In the following section we will investigate the nonlinear response of a bilayer graphene in the process of third order harmonic generation under the influence of laser field in nonadiabatic regime $\gamma \simeq 1$ with the frequencies in terahertz domain: $\omega = 0.03 \div 0.06$ eV/ \hbar .

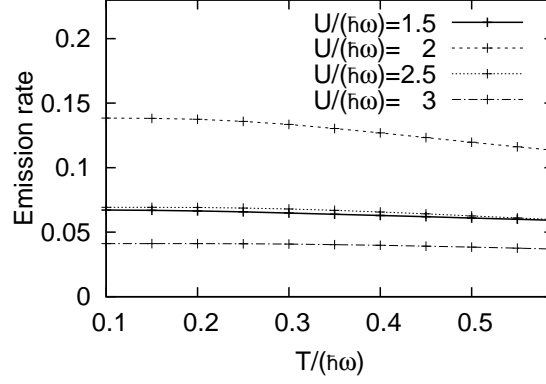


FIG. 6: 3rd harmonic emission rate in bilayer graphene J_3 (in arbitrary units) as a function of the temperature scaled to photon energy for various band gaps. The wave intensity defines by parameter $\chi = 1$ and frequency $\omega = 0.05$ eV/ \hbar .

III. NUMERICAL SIMULATIONS FOR THIRD ORDER HARMONIC GENERATION IN GAPPED BILAYER GRAPHENE

As was mentioned in Section II, at the multiphoton resonant excitation and particle-hole annihilation from the coherent superposition states the intense coherent radiation of the harmonics of the applied EM wave will occur. Here we consider the possibility of harmonic generation from the multiphoton excited states depending on the pump field intensity, created energy gap in a bilayer graphene, and temperature of the initial stationary state. The coherent part of the radiation spectrum we present by the mean value of the current density operator in the form:

$$j_\zeta = -eg_s \langle \widehat{\Psi}(\mathbf{r}, t) | \widehat{\mathbf{v}}_\zeta | \widehat{\Psi}(\mathbf{r}, t) \rangle. \quad (23)$$

Here $g_s = 2$ is the spin degeneracy factor, $\widehat{\mathbf{v}}_\zeta$ is the velocity given by (36), (37) in the Appendices.

Using the Eqs. (23), (36), (37) and (17), the expectation value of the current for the valley ζ can be written in the form:

$$\begin{aligned} \mathbf{j}_\zeta(t) = & -\frac{g_s e}{(2\pi\hbar)^2} \int d\mathbf{p} \{ \mathbf{V}(\mathbf{p}) (N_c(\mathbf{p}, t) - N_v(\mathbf{p}, t)) \\ & + 2\hbar^{-1} i \mathcal{E}_1(\mathbf{p}) [\mathbf{D}_t(\mathbf{p}) P^*(\mathbf{p}, t) - \mathbf{D}_t^*(\mathbf{p}) P(\mathbf{p}, t)] \}, \end{aligned} \quad (24)$$

where

$$\mathbf{V}(\mathbf{p}) = \frac{v_3 \mathbf{p} - 3\zeta \frac{v_3 p}{2m} \mathbf{p} \cos 3\vartheta + 3\zeta \frac{v_3 p^3}{2m} \sin 3\vartheta \frac{\partial \vartheta}{\partial \mathbf{p}} + 2 \frac{\mathbf{p}^3}{(2m)^2}}{\mathcal{E}_1(\mathbf{p})} \quad (25)$$

is the intraband velocity. The total current is composed from two terms with $N_c(\mathbf{p}, t)$ and $P(\mathbf{p}, t)$ which provide two sources for the generation of harmonics -inraband and interband, respectively. Interband high harmonics are radiated as a result of pump field-induced recombination of accelerated electron-hole pairs. Intraband high harmonics are generated as a result of the independent motion of carriers in their respective bands. Note that the relative contribution of intraband and interband high harmonics strongly depends on the nanostructure's material and pump field parameters. And the contributions of both mechanisms are essential when the energy gap is small compared with the wave photon energy [52].

Since there is no degeneracy upon valley quantum number ζ , the total current is obtained by a summation over ζ , and the last has the form:

$$j_x = j_{1,x} + j_{-1,x}; \quad (26)$$

$$j_y = j_{1,y} + j_{-1,y}.$$

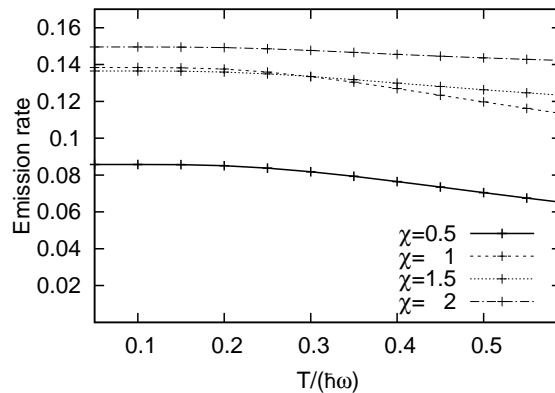


FIG. 7: 3rd harmonic emission rate in bilayer graphene J_3 (in arbitrary units) as a function of the temperature scaled to photon energy for various intensities. The wave frequency is $\omega = 0.05$ eV/ \hbar , band gap energy $U = 0.1$ eV.

The scaled total current components are the functions:

$$\frac{j_{x,y}}{j_0} = J_{x,y} \left(\omega t, \chi, \gamma, \frac{\mathcal{E}_L}{\hbar\omega}, \frac{T}{\hbar\omega}, \frac{U}{\hbar\omega} \right), \quad (27)$$

where $j_0 = \pi^{-2}e\omega\sqrt{m\omega/\hbar}$, J_x and J_y are the dimensionless periodic functions in case of monochromatic wave. They parametrically depend on the interaction parameters χ (1), γ (2), scaled Lifshitz energy, temperature and gap energy. Thus, having solutions of Eqs. (29)-(31), and making an integration in Eqs. (24), (25) one can calculate the n th harmonic radiation spectra with the help of a Fourier transform of the function $J_{x,y}(t)$. The emission rate of the n th harmonic is proportional to $n^2|j_n|^2$, where

$$|j_n|^2 = |j_{xn}|^2 + |j_{yn}|^2. \quad (28)$$

Here j_{xn} and j_{yn} are n th Fourier components of the field-induced total current for which the fast Fourier transform algorithm has been used. For the all plots one has used the normalized current density (27).

For the clarification of the harmonics generation due to multiphoton resonant excitation and particle-hole annihilation, from the coherent superposition states at $\gamma \simeq 1$ initially we examine the emission rate of the third harmonic. The fixed pump wave frequency is taken from terahertz domain in Figs. 3-7. The emission rate dependence versus pump wave strength defined by fixed value of parameter $\chi = 1$ is demonstrated in Fig. 3 for various gap energies. As is seen from this figure, for the field intensities $\chi \gtrsim 1$ at the gap energy $U \approx 0.1$ eV we have a strong deviation from power law for the emission rate of the third harmonic (in accordance with the perturbation theory $\sim \chi^3$). In Fig. 4 the dependence of emission rate on the energy gap is shown versus pump wave intensity and gap energy at room temperature. In Fig. 5 third harmonic emission rate is assumed as a function of the energy gap at various intensities defined by χ at the same wave frequency. As a result, we find the optimal parameters when the third harmonic emission rate is significant: $U \approx 0.1$ eV and at the larger intensity for the considered wave frequency.

To show the temperature dependence of the harmonic generation process at the resonant excitation, in Figs. 6, 7 the third harmonic coherent emission rate in bilayer graphene for various gap energies and various wave intensities are plotted at the fixed wave frequency $\omega = 0.05$ eV/ \hbar . The Fig. 6 shows that at the fixed pump wave intensity for a case of the found optimal value $U \approx 0.1$ eV, the third harmonic emission rate is suppressed with increasing of the temperature. And, as is seen from Fig. 7, at the same value $U \approx 0.1$ eV, with the temperature increase the emission rate of the third harmonic is strictly diminished, as in intrinsic bilayer graphene at $U = 0$ [9] for a small intensity only. The similar calculations for the intense pump wave or large gap energy U ($U \gg T$) have shown that emission rate exhibits a tenuous dependence on the temperature.

So, in accordance to the results of Figs. 3-7, an intense radiation of the third harmonic at the pump-wave-induced particle or hole acceleration and annihilation in gapped graphene can be obtained at room temperatures with the pump wave frequency in terahertz domain.

IV. CONCLUSION

We find out the real/optimal values of energy gap produced by a constant electric field, a wave intensity, and graphene temperature for the third harmonic coherent radiation, using the microscopic quantum theory of nonlinear interaction of a strong coherent radiation with a gapped bilayer graphene. The band gap in this system is produced by a constant electric field applied perpendicular to the surface of bilayer graphene. The closed set of differential equations for the single-particle density matrix was solved numerically for a gapped bilayer graphene in the vicinity of the ζK points in the Brillouin zone, in nonadiabatic regime of interaction when the Keldysh parameter is of the order of unity. In particular, the obtained results for the third order harmonic generation show that optimal values of characteristic parameters of the considering system make a gapped bilayer graphene an effective medium for third-order nonlinear optical effects at room temperatures for the pump wave frequencies in the terahertz and far infrared domains.

V. APPENDIX

Here we present the set of differential equations for the quantities $N_c(\mathbf{p}, t)$, $N_v(\mathbf{p}, t)$, $P(\mathbf{p}, t)$ and final relations for the transition dipole moment components and velocity operator. Thus, we need to solve the closed set of differential equations for the following quantities:

$$i\hbar \frac{\partial N_c(\mathbf{p}, t)}{\partial t} - i\hbar e \mathbf{E}(t) \frac{\partial N_c(\mathbf{p}, t)}{\partial \mathbf{p}} =$$

$$\mathbf{E}(t) \mathbf{D}_t(\mathbf{p}) P^*(\mathbf{p}, t) - \mathbf{E}(t) \mathbf{D}_t^*(\mathbf{p}) P(\mathbf{p}, t), \quad (29)$$

$$i\hbar \frac{\partial N_v(\mathbf{p}, t)}{\partial t} - i\hbar e \mathbf{E}(t) \frac{\partial N_v(\mathbf{p}, t)}{\partial \mathbf{p}} =$$

$$- \mathbf{E}(t) \mathbf{D}_t(\mathbf{p}) P^*(\mathbf{p}, t) + \mathbf{E}(t) \mathbf{D}_t^*(\mathbf{p}) P(\mathbf{p}, t), \quad (30)$$

$$i\hbar \frac{\partial P(\mathbf{p}, t)}{\partial t} - i\hbar e \mathbf{E}(t) \frac{\partial P(\mathbf{p}, t)}{\partial \mathbf{p}} =$$

$$[2\mathcal{E}_1(\mathbf{p}) + \mathbf{E}(t) \mathbf{D}_m(\mathbf{p}) - i\hbar \Gamma] P(\mathbf{p}, t)$$

$$+ \mathbf{E}(t) \mathbf{D}_t(\mathbf{p}) [N_v(\mathbf{p}, t) - N_c(\mathbf{p}, t)], \quad (31)$$

Taking into account Eq. (15) with the spinor wave functions (6) we obtain the transition dipole moment components in the ultimate forms:

$$D_{tx}(\mathbf{p}) = - \frac{e\hbar}{2\mathcal{E}_1(\mathbf{p}) \sqrt{\mathcal{E}_1^2(\mathbf{p}) - \frac{U^2}{4}}} \times \left(\left[\left(\frac{p^2}{2m} - mv_3^2 \right) \frac{\zeta p_y}{m} + \frac{v_3}{m} p_x p_y \right] - i \frac{U}{2\mathcal{E}_1} \left\{ \left(\frac{p^2}{2m} + mv_3^2 \right) \frac{p_x}{m} - \frac{3\zeta v_3}{2m} (p_x^2 - p_y^2) \right\} \right), \quad (32)$$

$$D_{ty}(\mathbf{p}) = - \frac{e\hbar}{2\mathcal{E}_1(\mathbf{p}) \sqrt{\mathcal{E}_1^2(\mathbf{p}) - \frac{U^2}{4}}}$$

$$\begin{aligned} & \times \left(\left[\left(-\frac{p^2}{2m} + mv_3^2 \right) \frac{\zeta p_x}{m} + \frac{v_3}{2m} (p_x^2 - p_y^2) \right] \right. \\ & \left. - i \frac{U}{2\mathcal{E}_1} \left\{ \left(\frac{p^2}{2m} + mv_3^2 \right) \frac{p_y}{m} + \frac{3\zeta v_3}{m} p_x p_y \right\} \right). \end{aligned} \quad (33)$$

Using Eq. (15), the total mean dipole moments $D_{x,ym}(\mathbf{p}) = D_{x,ym}(1, \mathbf{p}) - D_{x,ym}(-1, \mathbf{p})$ can be represented as:

$$\begin{aligned} D_{xm}(\mathbf{p}) &= -\frac{e\hbar U}{2\mathcal{E}_1(\mathbf{p}) \left(\mathcal{E}_1^2(\mathbf{p}) - \frac{U^2}{4} \right)} \\ & \times \left[\left(\frac{p^2}{2m} - mv_3^2 \right) \frac{\zeta p_y}{m} + \frac{v_3}{m} p_x p_y \right], \end{aligned} \quad (34)$$

$$\begin{aligned} D_{ym}(\mathbf{p}) &= -\frac{e\hbar U}{2\mathcal{E}_1(\mathbf{p}) \left(\mathcal{E}_1^2(\mathbf{p}) - \frac{U^2}{4} \right)} \\ & \times \left[\left(-\frac{p^2}{2m} + mv_3^2 \right) \frac{\zeta p_x}{m} + \frac{v_3}{2m} (p_x^2 - p_y^2) \right]. \end{aligned} \quad (35)$$

The velocity operator is defined by the relation $\hat{v}_\zeta = \partial \hat{H} / \partial \hat{\mathbf{p}}$. After the simple calculations for the effective 2×2 Hamiltonian (3), the velocity operator in components can be presented by the expressions:

$$\hat{v}_{\zeta x} = \zeta \begin{pmatrix} 0 & -\frac{1}{m} (\zeta \hat{p}_x - i \hat{p}_y) + v_3 \\ -\frac{1}{m} (\zeta \hat{p}_x + i \hat{p}_y) + v_3 & 0 \end{pmatrix}, \quad (36)$$

$$\hat{v}_{\zeta y} = i \begin{pmatrix} 0 & \frac{1}{m} (\zeta \hat{p}_x - i \hat{p}_y) + v_3 \\ -\frac{1}{m} (\zeta \hat{p}_x + i \hat{p}_y) - v_3 & 0 \end{pmatrix}. \quad (37)$$

Acknowledgments

The authors are deeply grateful to prof. H. K. Avetissian for permanent discussions and valuable recommendations. This work was supported by the RA MES Science Committee.

-
- [1] K. S. Novoselov, A. K. Geim, S. V. Morozov, D. Jiang, Y. Zhang, S. V. Dubonos, I. V. Grigorieva, and A. A. Firsov, "Electric field effect in atomically thin carbon films", *Science* **306**(5696), 666–669 (2004), <http://dx.doi.org/10.1126/science.1102896>.
- [2] A. H. Castro Neto, F. Guinea, N. M. R. Peres, K. S. Novoselov, and A. K. Geim, "The electronic properties of graphene", *Rev. Mod. Phys.* **81**, 109–162 (2009), <http://dx.doi.org/10.1103/RevModPhys.81.109>.
- [3] M. I. Katsnelson, K. S. Novoselov, and A. K. Geim, "Chiral tunnelling and the Klein paradox in graphene", *Nature Phys.* **2**, 620–625 (2006), <http://dx.doi.org/10.1038/nphys384>.
- [4] V. V. Cheianov, V. I. Fal'ko, and B. L. Altshuler, "The focusing of electron flow and a Veselago lens in graphene p-n junctions", *Science* **315**, 1252–1254 (2007), <http://dx.doi.org/10.1126/science.1138020>.
- [5] C. L. Lu, C. P. Chang, Y. C. Huang, R. B. Chen, and M. L. Lin, "Influence of an electric field on the optical properties of few-layer graphene with AB stacking", *Phys. Rev. B* **73**, 144427(1)-144427(9) (2006), <http://dx.doi.org/10.1103/PhysRevB.73.144427>.
- [6] S. A. Mikhailov, K. Ziegler, "Nonlinear EM response of graphene: frequency multiplication and the self-consistent-field effects", *J. Phys. Condens. Matter* **20**, 384204(1)-384204(10) (2008), <http://dx.doi.org/10.1088/0953-8984/20/38/384204/meta>.
- [7] H. K. Avetissian, A. K. Avetissian, G. F. Mkrtchian, K. V. Sedrakian, "Creation of particle-hole superposition states in graphene at multiphoton resonant excitation by laser radiation", *Phys. Rev. B* **85**, 115443(1)-115443(10) (2012), <http://dx.doi.org/10.1103/PhysRevB.85.115443>.

- [8] H. K. Avetissian, A. K. Avetissian, G. F. Mkrtchian, Kh. V. Sedrakian, “Multiphoton resonant excitation of Fermi-Dirac sea in graphene at the interaction with strong laser fields”, *J. Nanophoton.* **6**, 061702(1)-061702(17) (2012), <http://dx.doi.org/10.1117/1.JNP.6.061702>.
- [9] H. K. Avetissian, G. F. Mkrtchian, K. G. Batrakov, S. A. Maksimenko, A. Hoffmann, “Multiphoton resonant excitations and high-harmonic generation in bilayer grapheme”, *Phys. Rev. B.* **88**, 165411(1)-165411(9) (2013), <http://dx.doi.org/10.1103/PhysRevB.88.165411>.
- [10] H. K. Avetissian, G. F. Mkrtchian, K. G. Batrakov, S. A. Maksimenko, A. Hoffmann, “Nonlinear theory of graphene interaction with strong laser radiation beyond the Dirac cone approximation: Coherent control of quantum states in nano-optics”, *Phys. Rev. B* **88**, 245411(1)-245411(7) (2013), <http://dx.doi.org/10.1103/PhysRevB.88.245411>.
- [11] H. K. Avetissian, G. F. Mkrtchian, K. G. Batrakov, and S. A. Maksimenko, “Nonlinear interaction of coherent radiation with bilayer graphene and high harmonic generation”, In *Physics, Chemistry and Applications of Nanostructures*, World Scientific Publishing pp. 195-198 (2013), http://dx.doi.org/10.1142/9789814460187_0048.
- [12] H. K. Avetissian, G. F. Mkrtchian, “Coherent nonlinear optical response of graphene in the quantum Hall regime”, *Phys. Rev. B* **94**, 045419(1)-045419(7) (2016), <https://dx.doi.org/10.1103/PhysRevB.94.045419>.
- [13] P. Bowlan, E. Martinez-Moreno, K. Reimann, T. Elsaesser, and M. Woerner, “Ultrafast terahertz response of multilayer graphene in the nonperturbative regime”, *Phys. Rev. B* **89**, 041408(1)-041408(5) (2014), <https://dx.doi.org/10.1103/PhysRevB.89.041408>.
- [14] I. Al-Naib1, J. E. Sipe and M. M. Dignam, “Nonperturbative model of harmonic generation in undoped graphene in the terahertz regime”, *New J. Phys.* **17**, 113018(1)-113018(17) (2015), <http://dx.doi.org/10.1088/1367-2630/17/11/113018>.
- [15] L. A. Chizhova, F. Libisch, J. Burgdorfer, “Nonlinear response of graphene to a few-cycle terahertz laser pulse: Role of doping and disorder”, *Phys. Rev. B* **94**, 075412(1)-075412(10) (2016), <http://dx.doi.org/10.1103/PhysRevB.94.075412>.
- [16] D. Dimitrovski, L. B. Madsen, T. G. Pedersen, “High-order harmonic generation from gapped graphene”, *Phys. Rev. B* **95**, 035405(1)-035405(9) (2017), <https://dx.doi.org/10.1103/PhysRevB.95.035405>.
- [17] N. Yoshikawa, T. Tamaya, K. Tanaka, “High-harmonic generation in graphene enhanced by elliptically polarized light excitation”, *Science* **356**, 736-738 (2017), <http://dx.doi.org/10.1126/science.aam8861>.
- [18] H. K. Avetissian, A.G. Ghazaryan, G. F. Mkrtchian, K. V. Sedrakian, “High harmonic generation in Landau-quantized graphene subjected to a strong EM radiation”, *J. Nanophoton.* **11**, 016004(1)-016004(9) (2017), <http://dx.doi.org/10.1117/1.JNP.11.016004>.
- [19] H. K. Avetissian, G.F. Mkrtchian, “Impact of electron-electron Coulomb interaction on the high harmonic generation process in graphene”, *Phys. Rev. B* **97**, 115454(1)-115454(9) (2018), <http://dx.doi.org/10.1103/PhysRevB.97.115454>.
- [20] A. K. Avetissian, A.G. Ghazaryan, K. V. Sedrakian, and B. R. Avchyan, “Induced nonlinear cross sections of conductive electrons scattering on the charged impurities in doped graphene”, *J. Nanophoton.* **11**, 036004(1)-036004(11) (2017), <https://doi.org/10.1117/1.JNP.11.036004>.
- [21] A. K. Avetissian, A.G. Ghazaryan, K. V. Sedrakian, and B. R. Avchyan, “Microscopic nonlinear quantum theory of absorption of strong EM radiation in doped graphene”, *J. Nanophoton.* **12**, 016006(1)-016006(12) (2018), <https://doi.org/10.1117/1.JNP.12.016006>.
- [22] H. Liu, Y. Li, Y. S. You, Sh. Ghimire, T. F. Heinz, and D. A. Reis, “High-harmonic generation from an atomically thin semiconductor”, *Nature Physics* **13**, 262–265 (2017), <https://doi.org/10.1038/nphys3946>.
- [23] Sh. Ghimire and D. A. Reis “High-harmonic generation from solids”, *Nature Physics* **15**, 10–16 (2019), <https://doi.org/10.1038/s41567-018-0315-5>.
- [24] H. K. Avetissian, “Relativistic Nonlinear Electrodynamics”, The QED vacuum and matter in super-strong radiation fields, Springer, the Netherlands, 2016.
- [25] E. V. Castro, K. S. Novoselov, S. V. Morozov, N. M. R. Peres, J. M. B. Lopes dos Santos, J. Nilsson, F. Guinea, A. K. Geim, and A. H. Castro Neto, “Biased bilayer graphene: semiconductor with a gap tunable by the electric field effect”, *Phys. Rev. Lett.* **99**, 216802(1)-216802(4) (2007), <https://doi.org/10.1103/PhysRevLett.99.216802>.
- [26] Y. B. Zhang, T.-T. Tang, C. Girit, Z. Hao, M. C. Martin, A. Zettl, M. F. Crommie, Y. R. Shen, and F. Wang, “Direct observation of a widely tunable bandgap in bilayer graphene”, *Nature* **459**, 820–823 (2009), <https://doi.org/10.1038/nature08105>.
- [27] F. Guinea, A. H. C. Neto, N. M. R. Peres, “Electronic states and Landau levels in graphene stacks”, *Phys. Rev. B* **73**, 245426(1)-245426(8) (2006), <https://doi.org/10.1103/PhysRevB.73.245426>.
- [28] E. McCann and V. I. Fal’ko, “Landau-level degeneracy and quantum Hall effect in a graphite bilayer”, *Phys. Rev. Lett.* **96**, 086805(1)-086805(4) (2006), <https://doi.org/10.1103/PhysRevLett.96.086805>.
- [29] M. Koshino and T. Ando, “Transport in bilayer graphene: Calculations within a self-consistent Born approximation”, *Phys. Rev. B* **73**, 245403(1)-245403(8) (2006), <https://doi.org/10.1103/PhysRevB.73.245403>.
- [30] M. Tonouchi, “Cutting-edge terahertz technology”, *Nat. Photon.* **1**, 97–105 (2007), <https://doi.org/10.1038/nphoton.2007.3>.
- [31] S. Latil, L. Henrard, “Charge carriers in few-layer graphene films”, *Phys. Rev. Lett.* **97**, 036803(1)-036803(4) (2006), <https://doi.org/10.1103/PhysRevLett.97.036803>.
- [32] H. K. Min, A. H. MacDonald, “Electronic structure of multilayer graphene”, *Prog. Theor. Phys. Suppl.* **176**, 227–252 (2008), <https://doi.org/10.1143/PTPS.176.227/1883294>.
- [33] M. Aoki, H. Amawashi, “Dependence of band structures on stacking and field in layered graphene”, *Solid State Commun.* **142**, 123–127 (2007), <https://doi.org/10.1016/j.ssc.2007.02.013>.
- [34] S. B. Kumar, J. Guo, “Multilayer graphene under vertical electric field”, *Appl. Phys. Lett.* **98**, 222101(1)-222101(3) (2011), <https://doi.org/10.1063/1.3595335>.

- [35] K. Tang, R. Qin, J. Zhou, H. Qu, J. Zheng, R. Fei, H. Li, Q. Zheng, Z. Gao, and J. Lu, “Electric-field-induced energy gap in few-layer graphene”, *J. Phys. Chem. C* **115**, 9458–9464 (2011), <https://doi.org/10.1021/jp201761p>.
- [36] K. F. Mak, J. Shan, and T. F. Heinz, “Electronic structure of few-layer graphene: Experimental demonstration of strong dependence on stacking sequence”, *Phys. Rev. Lett.* **104**, 176404(1)-176404(4) (2010), <https://doi.org/10.1103/PhysRevLett.104.176404>.
- [37] D. S. L. Abergel and T. Chakraborty, “Generation of valley polarized current in bilayer graphene”, *Appl. Phys. Lett.* **95**, 062107(1)-062107(3) (2009), <https://doi.org/10.1063/1.3205117>.
- [38] E. Suarez Morell and L. E. F. Foa Torres, “Radiation effects on the electronic properties of bilayer graphene”, *Phys. Rev. B* **86**, 125449(1)-125449(5) (2012), <https://doi.org/10.1103/PhysRevB.86.125449>.
- [39] J. J. Dean and H. M. van Driel, “Graphene and few-layer graphite probed by second-harmonic generation: Theory and experiment”, *Phys. Rev. B* **82**, 125411(1)-125411(10) (2010), <https://doi.org/10.1103/PhysRevB.82.125411>.
- [40] S. Wu, L. Mao, A. M. Jones, W. Yao, C. Zhang, and X. Xu, “Quantum-enhanced tunable second-order optical nonlinearity in bilayer graphene”, *Nano Lett.* **12**, 2032–2036 (2012), <https://doi.org/10.1021/nl300084j>.
- [41] Y. S. Ang, S. Sultan, and C. Zhang, “Nonlinear optical spectrum of bilayer graphene in the terahertz regime”, *Appl. Phys. Lett.* **97**, 243110(1)-243110(3) (2010), <https://doi.org/10.1063/1.3527934>.
- [42] S. J. Brun, T. G. Pedersen, “Intense and tunable second-harmonic generation in biased bilayer graphene”, *Phys. Rev. B* **91**, 205405(1)-205405(8) (2015), <https://doi.org/10.1103/PhysRevB.91.205405>.
- [43] N. KuAngmar, J. Kumar, C. Gerstenkorn, R. Wang, H.-Y. Chiu, A. L. Smirl, and H. Zhao, “Third harmonic generation in graphene and few-layer graphite films”, *Phys. Rev. B* **87**, 121406(1)-121406(5) (2013), <https://doi.org/10.1103/PhysRevB.87.121406>.
- [44] T. Ohta, A. Bostwick, T. Seyller, K. Horn, and E. Rotenberg, “Controlling the electronic structure of bilayer graphene”, *Science* **313**, 951-954 (2006), <https://doi.org/10.1126/science.1130681>.
- [45] J. B. Oostinga, H. B. Heersche, X. L. Liu, A. F. Morpurgo, and L. M. K. Vandersypen, “Gate-induced insulating state in bilayer graphene devices”, *Nature Mater.* **7**, 151–157 (2008), <https://doi.org/10.1038/nmat2082>.
- [46] K. F. Mak, C. H. Lui, J. Shan, and T. F. Heinz, “Observation of an electric-field-induced band gap in bilayer graphene by infrared spectroscopy”, *Phys. Rev. Lett.* **102**, 256405(1)-256405(4) (2009), <https://doi.org/10.1103/PhysRevLett.102.256405>.
- [47] A. B. Kuzmenko, I. Crassee, D. van der Marel, P. Blake, and K. S. Novoselov, “Determination of the gate-tunable band gap and tight-binding parameters in bilayer graphene using infrared spectroscopy”, *Phys. Rev. B* **80**, 165406(1)-165406(12) (2009), <https://doi.org/10.1103/PhysRevB.80.165406>.
- [48] F. N. Xia, D. B. Farmer, Y. M. Lin, and P. Avouris, “Graphene field-effect transistors with high on/off current ratio and large transport band gap at room temperature”, *Nano Lett.* **10**, 715–718 (2010), <https://doi.org/10.1021/nl9039636>.
- [49] Z. Q. Li, E. A. Henriksen, Z. Jiang, Z. Hao, M. C. Martin, P. Kim, H. L. Stormer, and D. N. Basov, “Band structure asymmetry of bilayer graphene revealed by infrared spectroscopy”, *Phys. Rev. Lett.* **102**, 037403(1)-037403(4) (2009), <https://doi.org/10.1103/PhysRevLett.102.037403>.
- [50] A. B. Kuzmenko, E. van Heumen, D. van der Marel, P. Lerch, P. Blake, K. S. Novoselov, and A. K. Geim, “Infrared spectroscopy of electronic bands in bilayer graphene”, *Phys. Rev. B* **79**, 115441(1)-115441(5) (2009), <https://doi.org/10.1103/PhysRevB.79.115441>.
- [51] L. V. Keldysh, “Ionization in the field of a strong EM wave”, *Sov. Phys.-JETP* **20**, 1307-1313 (1965), http://www.jetp.ac.ru/cgi-bin/dn/e_020_05_1307.pdf.
- [52] H. K. Avetissian and G. F. Mkrtchian, “Higher harmonic generation by massive carriers in buckled two-dimensional hexagonal nanostructures”, *Phys. Rev. B* **99**, 085432(1)-085432(10) (2019), <https://doi.org/10.1103/PhysRevB.99.085432>.